arXiv:1003.4339v1 [cond-mat.mtrl-sci] 23 Mar 2010

Electron Paramagnetic Resonance of Boron Acceptors in Isotopically Purified Silicon

H. Tezuka,[1] A. R. Stegner,[2] A. M. Tyryshkin,[3] S. Shankar,[3]
M. L. W. Thewalt,[4] S. A. Lyon,[3] K. M. Itoh,[1,*] and M. S. Brandt[2]

[1] *School of Fundamental Science and Technology, Keio University, Yokohama 223-8522, Japan*
[2] *Walter Schottky Institut, Technische Universität München, Am Coulombwall 3, 85748 Garching, Germany*
[3] *Department of Electrical Engineering, Princeton University, Princeton, NJ 08544, USA*
[4] *Department of Physics, Simon Fraser University, Burnaby, British Columbia, Canada V5A 1S6*

(Dated: March 24, 2010)

The electron paramagnetic resonance (EPR) linewidths of B acceptors in Si are found to reduce dramatically in isotopically purified ^{28}Si single crystals. Moreover, extremely narrow substructures in the EPR spectra are visible corresponding to either an enhancement or a reduction of the absorbed microwave on resonance. The origin of the substructures is attributed to a combination of simultaneous double excitation and spin relaxation in the four level spin system of the acceptors. A spin population model is developed which qualitatively describes the experimental results.

Boron is the most widely employed shallow acceptor in silicon. However, due to the existence of four degenerate energy levels originating from the light and heavy hole bands (shown in Fig. 1 (a)) and their strong sensitivity to perturbations like internal strain [1], B exhibits rich optical and electron paramagnetic resonance (EPR) spectra, which are still not fully understood. Recently, some open questions associated with the optical properties of this acceptor have been solved due to the availability of isotopically enriched Si [2, 3]. Using such samples, it has been shown that the random distribution of the different host Si isotopes causes a residual acceptor ground state splitting in natural Si which is experimentally observed in the photoluminescence (PL) spectra of acceptor bound excitons [4] and also gives rise to inhomogeneous broadening of the infrared absorption spectra [5, 6].

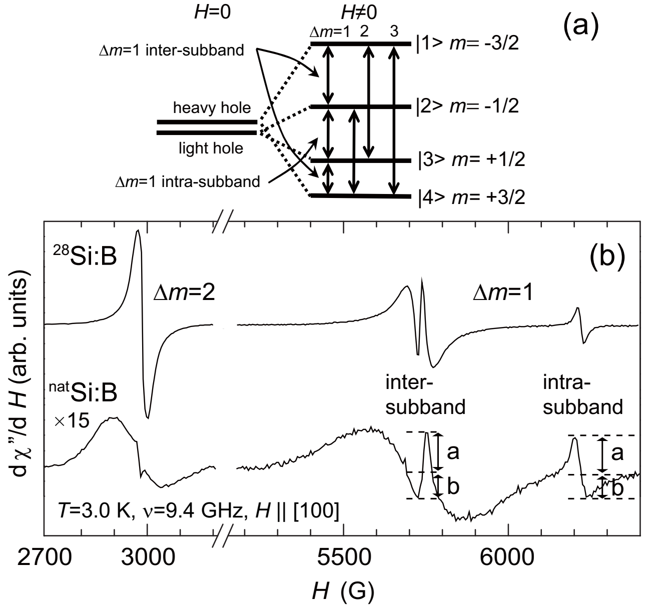

FIG. 1: (a) The level schemes of B acceptors. An externally applied magnetic field splits the heavy (light) hole subband into two energy states $|\pm 3/2\rangle$ ($|\pm 1/2\rangle$). We refer to each level as $|1\rangle$-$|4\rangle$ in the order shown. On top of the EPR-allowed transitions defined by Δm=1, the experimentally observed nominally EPR-forbidden transitions Δm=2 and Δm=3 are also shown. (b) EPR spectra recorded at T=3.0 K on ^{28}Si:B and $^{\mathrm{nat}}$Si:B samples showing the Δm=1 and 2 transitions.

Similarly, host isotope effects might also account for various properties of the EPR spectra of B in Si that have not been understood so far. The first successful boron EPR required the application of large homogeneous external stress to diminish the influence of inhomogeneous internal strain fields that are mainly induced by randomly distributed point defects and dislocations. These defects lead to a statistical distribution of ground state splittings, which, depending on the defect concentration, can result in an extremely large inhomogeneous broadening of the EPR resonance lines in externally unstrained Si [7]. The first observation of boron EPR without external stress was finally realized in 1978 [8, 9], when Si crystal growth techniques had developed enough to obtain samples of sufficient crystalline quality. However, the experimentally observed EPR linewidths have always been much broader than could be explained solely by the residual defect concentrations in high quality Si. In addition, Neubrand observed sharp substructures in the main resonance peaks, with and without externally applied stress [8, 9]. More recent studies on acceptor EPR probing dependencies on temperature, external stress, and frequency [10, 11] found the same sharp features, but the origin of these substructures remained unclear.

Here, we present experimental evidence that indeed the random distribution of stable Si isotopes is the major cause of inhomogeneous broadening of boron EPR spectra in natural Si. Moreover, thanks to the sharpening of the main EPR lines, the improved visibility of the sharp substructures allows for detailed studies of their origin. The substructures are shown to arise from an interplay between simultaneous excitation of two EPR transitions and spin relaxation in the four level spin system of B acceptors in Si. A theoretical model based on this assumption is developed to describe the temperature dependence of the substructures.

The experiments were performed with two p-type Si single crystals. The first sample, referred to as $^{\mathrm{nat}}$Si:B, was float-zone grown, has a natural isotopic composition and a B concentration of 1.4×10^{14} cm^{-3}. The isotopically purified sample ($\simeq$99.98 % ^{28}Si), referred to as ^{28}Si:B, comes from the neck of a float-zone crystal and is doped with B to a concentration of $3(\pm1)\times10^{14}$ cm^{-3}.

EPR measurements at a temperature of T=1.8 K were performed using a Bruker E580 EPR spectrometer equipped with a flex-line resonator (ED-4118MD5) operating at a microwave frequency ν=9.6 GHz. An Oxford CF935 helium-flow cryostat was used to maintain the temperature. For experiments at $T\geq$2.8 K, a Bruker E500 spectrometer in conjunction with a super-high-Q resonator (ER-4122SHQE) was used at ν=9.4 GHz. In this case, the sample was cooled using an Oxford ESR900 helium-flow cryostat. Lock-in detection using magnetic field modulation leads to the detection of the first derivative $d\chi''/dH$ of the imaginary part of the magnetic susceptibility χ'' with respect to the magnetic field H. The absorption curves, which are proportional to χ'', are obtained via numerical integration of the measured spectra.

Figure 1 (b) shows two overview EPR spectra that were measured on the ^{28}Si:B and the $^{\mathrm{nat}}$Si:B samples. In both spectra, we observe three distinct B-related resonances. From the angular dependence of the effective g-values [8, 9], we assign the resonance at H=2980 G to a superposition of the two inter-subband Δm=2 transitions, where m is the magnetic quantum number of the total angular momentum J=3/2 of the B acceptor. The resonances at H=5730 G and H=6220 G originate from a superposition of the two inter-subband Δm=1 transitions $|1\rangle\leftrightarrow|2\rangle$ and $|3\rangle\leftrightarrow|4\rangle$ and the intra-subband Δm=1 transition $|2\rangle\leftrightarrow|3\rangle$, respectively [8, 9, 12]. The most prominent difference between the two spectra is the decreased linewidth of all B-related resonances in the isotopically purified sample. This effect is most strongly pronounced for inter-subband transitions. As found by PL in Ref. [4, 6], local fluctuations of the valence band edge due to the random distribution of the different Si isotopes are responsible for the residual splitting of the B acceptor ground state in $^{\mathrm{nat}}$Si in absence of an external magnetic field. A detailed modelling of the influence of the isotope-induced fluctuations on the EPR resonances shows that this effect also accounts quantitatively for the inhomogeneous broadening of B-related EPR signals that could not be explained by point defect-induced random strain fields. This is in marked difference to the broadening of donor EPR lines in Si, which is caused by superhyperfine interaction with ^{29}Si nuclei [13]. The quantitative investigation of the broadening mechanism in Si:B is beyond the scope of this paper and will be given elsewhere. Here, we focus on the origin of the sharp substructures that appear in the middle of the inter-subband resonances. The observation of these substructures in ^{28}Si:B establishes that they do not result from an isotopic effect.

Figure 2 shows the inter-subband resonances on an expanded magnetic field scale as measured for ^{28}Si:B at two different temperatures. The narrow substructure is observed in all four spectra. By cooling from 3.2 to 1.8 K, the linewidth of the substructures decreases substantially, from 15 to 3 G for Δm=1 and from 5 to 1 G for Δm=2. In contrast, the broad underlying signals show much weaker changes in linewidth with temperature (from 78 to 70 G for Δm=1, 36 to 35 G for Δm=2). Thus, even though the line shape of the broad resonances is Lorentzian, the lack of any significant temperature dependence suggests that the lines are inhomogeneously broadened. This broadening is attributed to the distribution of transition energies between different energy levels induced by random local strains, which are well accounted for by the $\sim1\times10^{16}$ cm^{-3} concentration of C impurities as measured by infrared absorption spectroscopy on the $\sim$607 cm^{-1} C local vibrational mode [9, 14].

The insets in Fig. 2 show the integrated absorption curves in the magnetic field region of the substructure. We observe the following experimental facts: (1) For the Δm=1 spectra (Fig. 2 (a)), the substructure has a negative sign corresponding to a decrease of the microwave absorption at the center of the broad resonance. The intensity of this dip increases with decreasing temperature. We have exclusively observed a negative sign of the substructure in the Δm=1 resonance for all temperatures

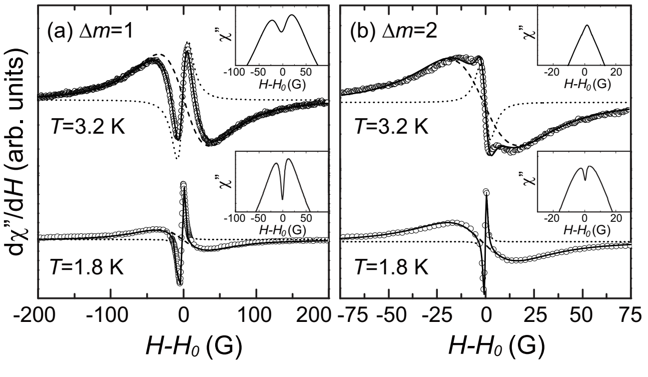

FIG. 2: EPR spectra of the inter-subband Δm=1 resonance (a) and the Δm=2 resonance (b) in ^{28}Si:B for $H||[100]$. The upper spectrum in each figure was measured at T=3.2 K, ν=9.38 GHz and a microwave power of P=0.2 mW. The lower spectra were measured at T=1.8K, ν=9.56 GHz and P=0.002 mW. The values of P were chosen to achieve the same microwave excitation rate w in the two resonators used. Solid lines show the results of numerical fittings composed of two Lorentzian lines, which are separately shown as dashed and dotted lines. H_0 is the resonance field of each signal. The amplitudes of the spectra were normalized. The insets show the integrated absorption spectra in the magnetic field region of the substructures in arbitrary units.

investigated. (2) In contrast, for the Δm=2 resonance, the microwave absorption in the substructure is enhanced at high temperatures, giving rise to a sharpened peak of the integrated spectrum measured at T=3.2 K. However, when the temperature is decreased to 1.8 K, the sign of the substructure line reverses, and a dip in the absorption spectrum is observed. (3) Microwave power saturation experiments (not shown) reveal that the saturation behavior of the substructure lines strongly deviates from that of the underlying broad signals; the relative intensity of the substructure decreases with increasing microwave power. No power broadening is observed for the substructure lines. (4) As has been pointed out in Ref. [8], the resonance fields of the substructure lines do not change when a small external stress is applied. (5) We find that the linewidths of the intra-subband Δm=1 resonance and the substructure of the inter-subband Δm=1 signal are very similar, in particular for temperatures below 3 K. Moreover, in the $^{\mathrm{nat}}$Si sample, for each orientation of H (not shown) these two resonances have the same asymmetry of the line shape, defined as the a/b ratio in Fig. 1(b), indicating that transitions between $|2\rangle$ and $|3\rangle$ are involved at least in the generation of the Δm=1 substructure.

The experimental observations summarized above strongly argue against a model assuming that the narrow substructure lines arise from a partial overlap of two asymmetric lineshapes, e.g. the $|1\rangle\leftrightarrow|2\rangle$ and $|3\rangle\leftrightarrow|4\rangle$ transitions in case of the Δm=1 signal, or the $|1\rangle\leftrightarrow|3\rangle$ and $|2\rangle\leftrightarrow|4\rangle$ transitions in case of the Δm=2 signal, as has been already speculated in Ref. [8]. On the other hand, a similar "substructure" line in the middle of a broad resonance has been reported for Ni^{2+} centers in MgO [15]. However, the cross-relaxation model invoked there can not account for the positive sign of the Δm=2 substructure observed here for $T\geq$3.2 K. In what follows, we demonstrate which interplay of spin excitation and relaxation in the four level system of Si:B causes the narrow substructure lines observed.

The centers of the broad resonances, where the substructure lines develop, correspond to B acceptors that experience a strain close to zero. In this case, the energy level scheme of the four level system is symmetric, as shown in the insets of Fig. 3, and the energies of the transitions $|1\rangle\leftrightarrow|2\rangle$ and $|3\rangle\leftrightarrow|4\rangle$ [$|1\rangle\leftrightarrow|3\rangle$ and $|2\rangle\leftrightarrow|4\rangle$] are equal, so that they are resonantly excited at the same time. This double excitation can lead to a change in the microwave absorption with respect to the situation when only one transition can be excited. The magnitude and sign of this change will depend on the ratios between relaxation and excitation rates in the level system.

To explore this scenario, we have performed a first calculation based on an incoherent spin population model [16, 17] composed of a set of rate equations. The time evolution of the spin population n_i of each state $|i\rangle$ is given by the sum of all possible excitation and relaxation terms. Relaxation and excitation rates from $|i\rangle$ to $|j\rangle$ are represented by γ_{ij} and w_{ij}, respectively.

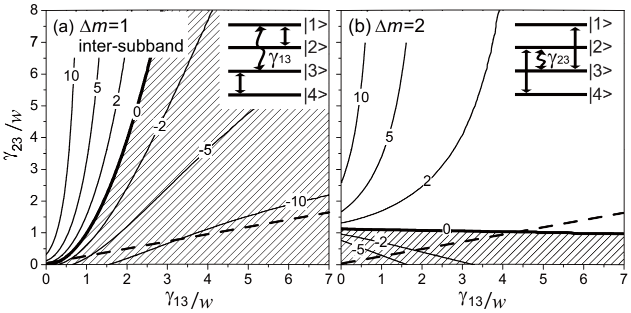

FIG. 3: Contour plots obtained by the population model described in the text for (a) Δm=1 and (b) Δm=2. The contour lines indicate a relative intensity (in %) of the substructure lines as compared to the intensity of the broad underlying transition. Negative and positive intensity corresponds to a suppression (dip) and an enhancement (peak) of the microwave power absorptions, respectively. The negative region is shown shaded. The parameters used in the calculation were T=3 K, ν=9.4 GHz, and γ_{14}/w=γ_{12}/w=1, with w being the resonant microwave excitation rate. The dashed line represents the assumed correlated temperature dependence of γ_{13} and γ_{23} in ^{28}Si:B as discussed in the text.

We use our model to compare the microwave absorption between exactly *on* and slightly *off resonance* conditions. For the *on resonance* condition where the substructure emerges, w_{12} and w_{34} [w_{13} and w_{24}] are assumed to have the same non-zero value w for the Δm=1 [Δm=2] resonance, while all the other elements in the excitation matrix are set to zero. The rate equations are solved for the steady state condition ($d\mathbf{n}/dt$=0) using the following assumptions: (i) Boltzmann balance of the relaxation rates, i.e. γ_{ji}=$\gamma_{ij}\exp(-\Delta E_{ij}/kT)$, where ΔE_{ij} is the energy difference between the states $|i\rangle$ and $|j\rangle$ and k is the Boltzmann constant. (ii) γ_{12}=γ_{34} and γ_{13}=γ_{24}, dictated by the symmetry of the Si:B Hamiltonian when the local strain is close to zero, (iii) w_{ji}=w_{ij}, required for magnetic dipole transitions, and (iv) $\sum_i n_i$=1 to conserve the total number of spins. The sum of the resulting population differences, (n_1-n_2)+(n_3-n_4) [(n_1-n_3)+(n_2-n_4)] for the Δm=1 [for Δm=2] transition, is used as a measure for the microwave absorption. To simulate the situation slightly *off resonance*, where double excitation is not possible, only one excitation at a time is allowed, e.g. $w_{12}\neq$0 [$w_{13}\neq$0] is assumed for the Δm=1 [Δm=2] resonance, and the microwave absorption represented by n_1-n_2 [n_1-n_3] is added to the microwave absorption n_3-n_4 [n_2-n_4] that is obtained by separately considering only the second transition with the excitation $w_{34}\neq$0 [$w_{24}\neq$0].

Results of such calculations are shown in contour plots in Fig. 3. The relative change of the microwave absorption due to double excitation, calculated as the population differences between exactly *on* and slightly *off resonance* conditions, is plotted as a function of the normalized relaxation rates γ_{13}/w and γ_{23}/w (all other relaxation rates were kept constant, e.g. $\gamma_{12}/w=\gamma_{14}/w=1$). This calculated change in absorption can be compared with the intensity of the substructure in Fig. 2. The open and shaded regions in Fig. 3 correspond to a suppression (dip substructure) and an enhancement (peak substructure) of microwave absorption, respectively. The dashed line shown in the plot corresponds to a constant ratio of $\gamma_{13}/\gamma_{23}=4/1$, motivated by the temperature independent ratio of substructure linewidths, $\Delta H_{\Delta m=1}/\Delta H_{\Delta m=2}\sim 4$, observed experimentally. Assuming all other parameters to only depend moderately on temperature, a variation of the temperature in our experiments can be viewed in a first approximation as a correlated change of γ_{13} and γ_{23} along the dashed line. This picture qualitatively explains the experimentally observed temperature dependence of the substructure line intensity in Fig. 2. For example, we find a negative sign (dip) for the $\Delta m=1$ substructure and a positive sign (peak) for the $\Delta m=2$ substructure when $\gamma_{13}/w\geq 4$ and $\gamma_{23}/w\geq 1$. Experimentally, this situation corresponds to temperatures $\geq$3.2 K. Upon decreasing both γ_{13}/w and γ_{23}/w along the dashed line, corresponding to lowering the temperature from 3.2 K to 1.8 K in the experiment, we observe a change of the sign for the $\Delta m=2$ substructure from positive to negative. For the $\Delta m=1$ substructure, the sign always stays negative for all γ_{13} and γ_{23} along the dashed curve, agreeing with the experimental finding that the sign is always negative at all accessible temperatures.

By simulating the model using a range of γ_{ij} parameters we have identified several requirements for the relative magnitude of the γ_{ij} in order to reproduce the experimental observations. First, to achieve a substantial effect (e.g. 10 %) from the double excitation requires that all γ_{ij} are of the same order of magnitude and also that the applied microwave power is close to saturation, i.e. $\gamma_{12}\sim\gamma_{13}\sim\gamma_{14}\sim\gamma_{23}\sim w$, as used in Fig. 3. Second, to observe a temperature dependent change of the sign for the $\Delta m=2$ substructure requires that $\gamma_{13}\geq\gamma_{12}$. This order of the γ_{ij} is unusual and contrasts with $\gamma_{12}\geq\gamma_{23}\gg\gamma_{13}\gg\gamma_{14}$ usually seen in other high-spin systems where zero-field splitting (ZFS) dominates spin relaxation [18]. However, we point out that the ZFS Hamiltonian in Si:B is represented by the S_i^3 terms [8] (in contrast to usual S_i^2), and therefore the order of relaxation rates can be different. The results presented here should therefore motivate the development of a detailed theory of relaxation effects in Si:B. Independent of this, we have performed microwave power saturation measurements (not shown) and confirmed that all resonances in Si:B saturate at about the same microwave power. The multiple relaxation pathways in the four level system make a direct interpretation of these saturation experiments difficult. Nevertheless, the fact that microwave power saturation occurs at the same power indicates that at least some of the γ_{ij} in Si:B have comparable magnitudes as assumed.

Our model is still somewhat qualitative and does not reproduce all experimental facts. For example, the model predicts that the strongest effect from double excitation should be seen at close to saturation conditions, i.e. $\gamma_{ij}/w\sim 1$, which is not in line with experiment. Further improvements to the model could be based on the density matrix formalism and the Redfield relaxation theory to construct the full set of Bloch equations for the $J=3/2$ spin system, also taking into account the specific spin Hamiltonian of Si:B to correctly predict the relaxation rates between different spin levels. Nevertheless, the instructive model constructed here establishes that the substructures in the EPR lines arise from the double excitation among the four levels of B acceptors. The improved understanding of the resonance properties of acceptors and the additional degree of freedom achieved via isotope engineering could make these valence band-derived states versatile competitors to the more thoroughly studied donors also in applications such as spin- or orbitronics.

The work at Keio was supported in part by the JST-DFG Strategic Cooperative Program on Nanoelectronics, in part by Grant-in-Aid for Scientific Research #18001002, by Special Coordination Funds for Promoting Science and Technology, and by a Grant-in-Aid for the Global Center of Excellence at Keio University. Work in Garching was supported by the JST-DFG program (Br 1585/5). Work at Princeton was supported by the NSA/LPS through LBNL (MOD 713106A).

---

[*] e-mail: kitoh@appi.keio.ac.jp

[1] W. Kohn, in *Solid State Physics*, ed. by F. Seitz and D. Turnbull (Academic Press, New York, 1957), vol. 5, p. 257.
[2] K. M. Itoh *et al.*, Jpn. J. Appl. Phys. **42**, 6248 (2003).
[3] K. Takyu *et al.*, Jpn. J. Appl. Phys. **38**, L1493 (1999).
[4] D. Karaiskaj *et al.*, Phys. Rev. Lett. **89**, 016401 (2002).
[5] D. Karaiskaj *et al.*, Phys. Rev. Lett. **90**, 186402 (2003).
[6] D. Karaiskaj *et al.*, Phys. Rev. Lett. **90**, 016404 (2003).
[7] G. Feher, C. J. Hensel, and E. A. Gere, Phys. Rev. Lett. **5**, 309 (1960).
[8] H. Neubrand, phys. stat. sol. (b) **86**, 269 (1978).
[9] H. Neubrand, phys. stat. sol. (b) **90**, 301 (1978).
[10] A. Köpf and K. Lassmann, Phys. Rev. Lett. **69**, 1580 (1992).
[11] H. Schad and K. Lassmann, Phys. Lett. **56A**, 409 (1976).
[12] J. M. Luttinger, Phys. Rev. **102**, 1030 (1956).
[13] G. Feher, Phys. Rev. **114**, 1219 (1959).
[14] P. G. Sennikov *et al.*, Semiconductors **39**, 300 (2005).
[15] S. R. P. Smith, F. Dravnieks, and J. E. Wertz, Phys. Rev. **178**, 471 (1969).
[16] A. Abragam, *The Principles of Nuclear Magnetism*, (Clarendon Press, Oxford, 1961)
[17] H. Shikata, Bull. Chem. Soc. Japan **50**, 3084 (1977).
[18] M. Rubinstein, A. Baram, and Z. Luz, Mol. Phys. **20**, 67, (1971).